Biosensors and Bioelectronics 26 (2010) 923–928

Contents lists available at ScienceDirect

Biosensors and Bioelectronics

journal homepage: www.elsevier.com/locate/bios

Short communication

Improved detection limits of toxic biochemical species based on impedance measurements in electrochemical biosensors

B.B. Narakathu [a], M.Z. Atashbar [a,*], B.E. Bejcek [b]

[a] Electrical and Computer Engineering, Western Michigan University, MI 49008, USA
[b] Biological Sciences, Western Michigan University, MI 49008, USA

ARTICLE INFO

Article history:
Received 8 April 2010
Received in revised form 12 June 2010
Accepted 26 June 2010
Available online 3 July 2010

Keywords:
Biosensor
Electrochemical
Interdigitated electrode
Impedance
Pico mole

ABSTRACT

An impedance based electrochemical biosensor was designed and fabricated for the detection of various chemical and biological species, with glass as substrate material and gold interdigitated electrodes. A flow cell with inlet and outlet ports for the microfluidic chamber was designed and fabricated using acrylic material with a reservoir volume of 78 μl. The feasibility of the fabricated sensor for detecting very low concentration of chemical and biological species was demonstrated. Electrochemical impedance spectroscopy (EIS) was employed as the detection technique. The impedance based response of the two-terminal device revealed a very high sensitivity with low concentrations of mouse monoclonal IgG, sarcosine, cadmium sulphide (CdS) and potassium chloride (KCl) at pico mole levels.

1. Introduction

A steady effort has been made on the development of efficient and easy-use electrochemical biosensors. Electrochemical biosensors with rapid and highly sensitive detection capabilities of various bio/chemical species are of great demand in the field of life sciences. Existing immuno assay techniques such as enzyme linked immuno assay (ELISA), fluoro immuno assay (FIA) and radio immuno assay (RIA) are expensive, laborious, cumbersome, hazardous and require specific labels for detection purposes thus making them more time consuming and complex (Muramatsu et al., 1987; Caruso et al., 1996; Wong et al., 2002). Developing easy-to-use electrochemical biosensors for detecting the concentration and activities of the various biological species therefore becomes very important.

The recent trend to miniaturize electrochemical biosensors is very fantasizing in the field of biosensors and has also been reported in many previous studies (Wang et al., 2005; Atashbar et al., 2005, 2006; Haes and Duyne, 2002; Basu et al., 2004; Vamvakaki and Chaniotakis, 2007; Vo-Dinh et al., 2001; Zou et al., 2007). The small size of the biosensors leads to very small-scale experiments which results in very low sample volume; i.e. to the extent of nanoliters, or even picoliters. Hand-held electrochemical devices with accuracy and sensitivity similar to that of bench-top analyzers have already been developed for certain applications. Although still at the basic research stage, many new applications are yet to be discovered. Improved modern fabrication techniques play a major role in developing these miniaturized devices.

Recently, the use of microelectrodes in electrochemical detection has also been receiving close attention in this field (Li et al., 2010; Bitziou et al., in press; Raina et al., 2010; Hu et al., 2010; Lupu et al., 2010; Antohe et al., 2009; Xu et al., 2009; Kim et al., 2009; Huffman and Venton, 2009; Lee et al., 2008; Zaouak et al., 2009; Qing et al., 2008; Xiang et al., 2007). Pioneering work was done on interdigitated array (IDA) electrodes by Sanderson and Anderson (1985) and several applications were reported (Chidsey et al., 1986; Fosdick et al., 1986; Feldman and Murray, 1986; Yang, 2008; Alocilja, 2008). The characteristics of the IDA electrodes and its applications in electrochemistry have been extensively studied (Tabei et al., 1994; Niwa et al., 1989; Horiuchi et al., 1992; Webster et al., 2009; Ochiai et al., 2009; Ah et al., 2006; Mannoor et al., 2010; Yi and Park, 2005; Cohen and Kunz, 2000). It was proved that the IDAs offer higher sensitivity than macroelectrodes.

In this work we have fabricated an efficient biosensor which incorporates gold (Au) interdigitated electrodes (IDT), using photolithography technique. Gold has been chosen as the electrode material for this work due to its inertness and because of its known affinity for biomolecules, especially for its ability to bind to proteins (Leuvering et al., 1980). The capability of the biosensor is exhibited through the quantitative detection of various chemical as well as biological substances like mouse monoclonal IgG, sarco-

* Corresponding author at: Department of Electrical and Computer Engineering, Western Michigan University, Parkview Campus 1903, W. Michigan Ave, Kalamazoo, MI 49008, USA. Tel.: +1 269 276 3148; fax: +1 269 276 3151.
E-mail address: massood.atashbar@wmich.edu (M.Z. Atashbar).

0956-5663/$ – see front matter © 2010 Elsevier B.V. All rights reserved.
doi:10.1016/j.bios.2010.06.051

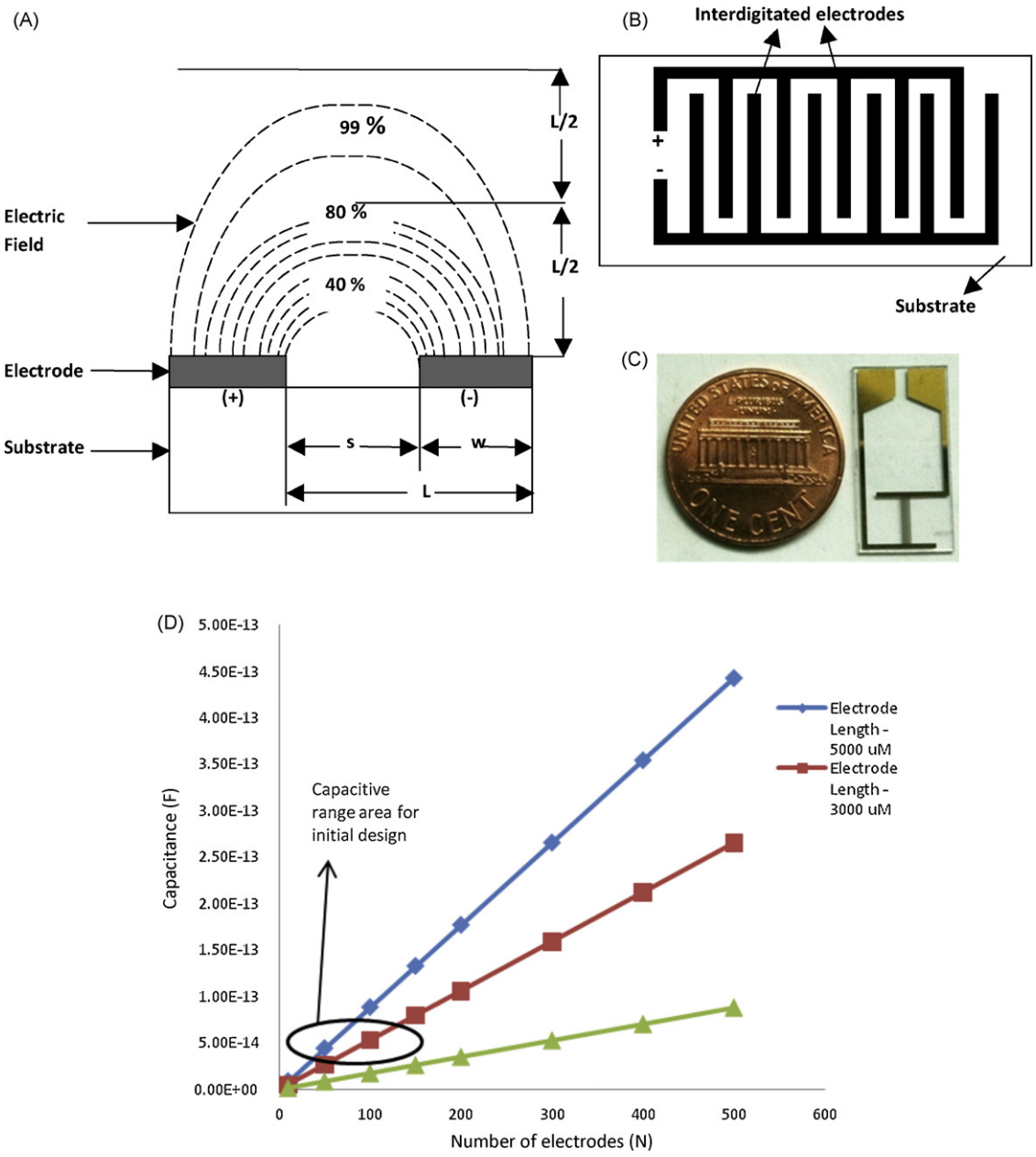

Fig. 1. (A) Working principle of interdigitated gold electrodes showing electric field, electrode width (*w*) and spacing (*s*). An 80% mark means that 80% of the current flows beneath that curve. (B) Geometry of interdigitated electrodes. (C) Photolithographically fabricated biosensor. (D) Calculated capacitance for varying number of electrodes (*N*) and electrode length (*L*).

sine, cadmium sulphide (CdS) and potassium chloride (KCl). A flow cell, with inlet and outlet ports for the microfluidic chamber, was also fabricated using acrylic material.

2. Experimental

2.1. Material, chemicals, antibody and sample preparation

Spring loaded small outline integrated chip (SOIC) test clips (14 pin) were purchased from Pomona Electronics. Tubing (inner diameter – 0.01 in.; outer diameter – 0.0625 in.) and tube connection accessories for sample transfer were purchased from Upchurch Scientific. CdS, KCl, sarcosine, phosphate buffer saline (PBS) (all in crystalline form) were purchased from Sigma–Aldrich Chemical Company. Mouse monoclonal IgG antibody was purchased from Bio-Design International Inc.

Sarcosine was mixed with PBS to form solutions of 1 pM and 100 pM concentrations. Mouse monoclonal IgG was resuspended in PBS to form 1 pM, 10 pM, 1 nM, 5 nM, 50 nM and 100 μM concentrations and stored at −20 °C in 10 ml aliquots before use. Distilled water (DI) was used to prepare 1 pM, 50 nM, 50 μM and 50 mM concentration solutions of CdS.

2.2. Design parameters and configuration

Several electrode geometries have been developed during the last few decades to lower the detection limit of electrochemical reactions and the use of microfabrication methods has led to the extensive use of microelectrode systems exploiting their high sensitivity in conjunction with simple device set up. Microelectrodes fabricated by lithographic technique on silicon and glass substrates have been of great interest, because they typically have a higher

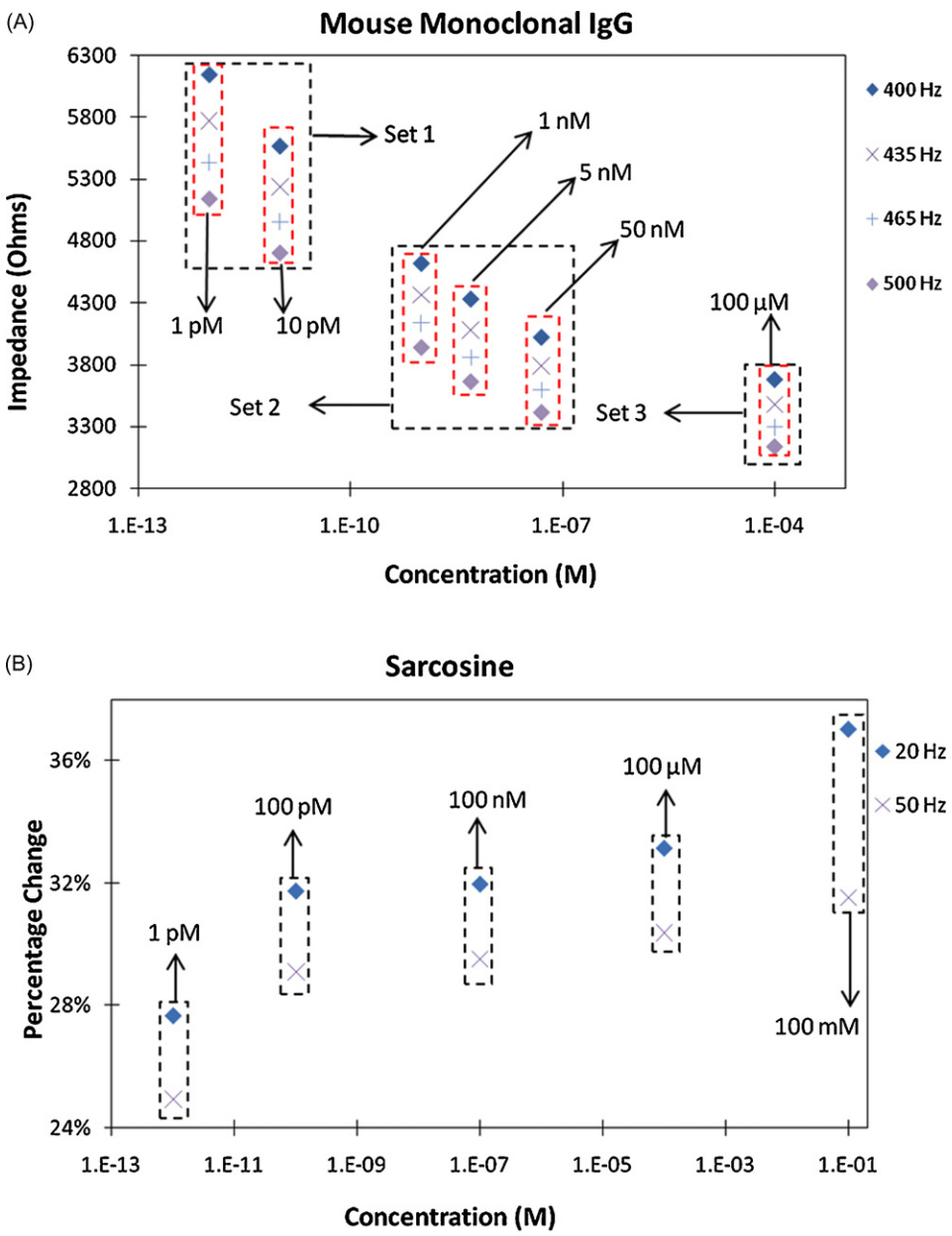

Fig. 2. Sensor response to (A) mouse IgG and (B) sarcosine at applied potential of 1 mV.

sensitivity than macroelectrodes of conventional size, since the macroelectrodes have a semi-infinite linear diffusion layer and thus a greater depletion of reactants in contrast to the microelectrodes, which have a spherical diffusion layer and therefore a greater rate of reactant supply. An interdigitated microelectrode array, which is one of the most prominent examples of microelectrodes, offers several advantages such as fast establishment of a steady-state signal, low ohmic drop of the potential, and increased signal-to-noise ratio. These advantages have led to the use of two-electrode circuits, rather than the conventional three-electrode potentiostatic circuits in wide use with macroelectrodes (Min and Baeummer, 2004).

Interdigitated electrode geometry has been used in this study as a sensing surface for analysis of the analytes. Research on optimization of interdigitated electrodes (Min and Baeummer, 2004) with respect to signal-to-noise ratio has shown that the key parameters associated with the interdigitated electrode geometry are the number of electrodes (N), electrode finger width (w), electrode finger spacing (s) and electrode height (h). It was proved that lower number of electrodes was superior to larger number of electrodes (200 vs. 400) at low concentrations of 50–100 µM. Also 1–5 µm wide electrodes were shown to be ideal as wider electrodes seem to lose some of the radial diffusion pattern known to be associated with microelectrodes. In addition better results were obtained with 5 µm electrode spacing. Optimum output signals were said to be obtained with electrode heights in the range of 70–140 nm. Studies (Gerwen et al., 1998) have also shown that nano-scaled electrodes with width and spacing from 500 nm down to 200 nm will only scan in a region (some 100 nm) above the surface and thus an improved sensitivity is obtained when compared to conventional electrodes (1 µm to millimeters). Results from the same study also demonstrated the current comprisement curves

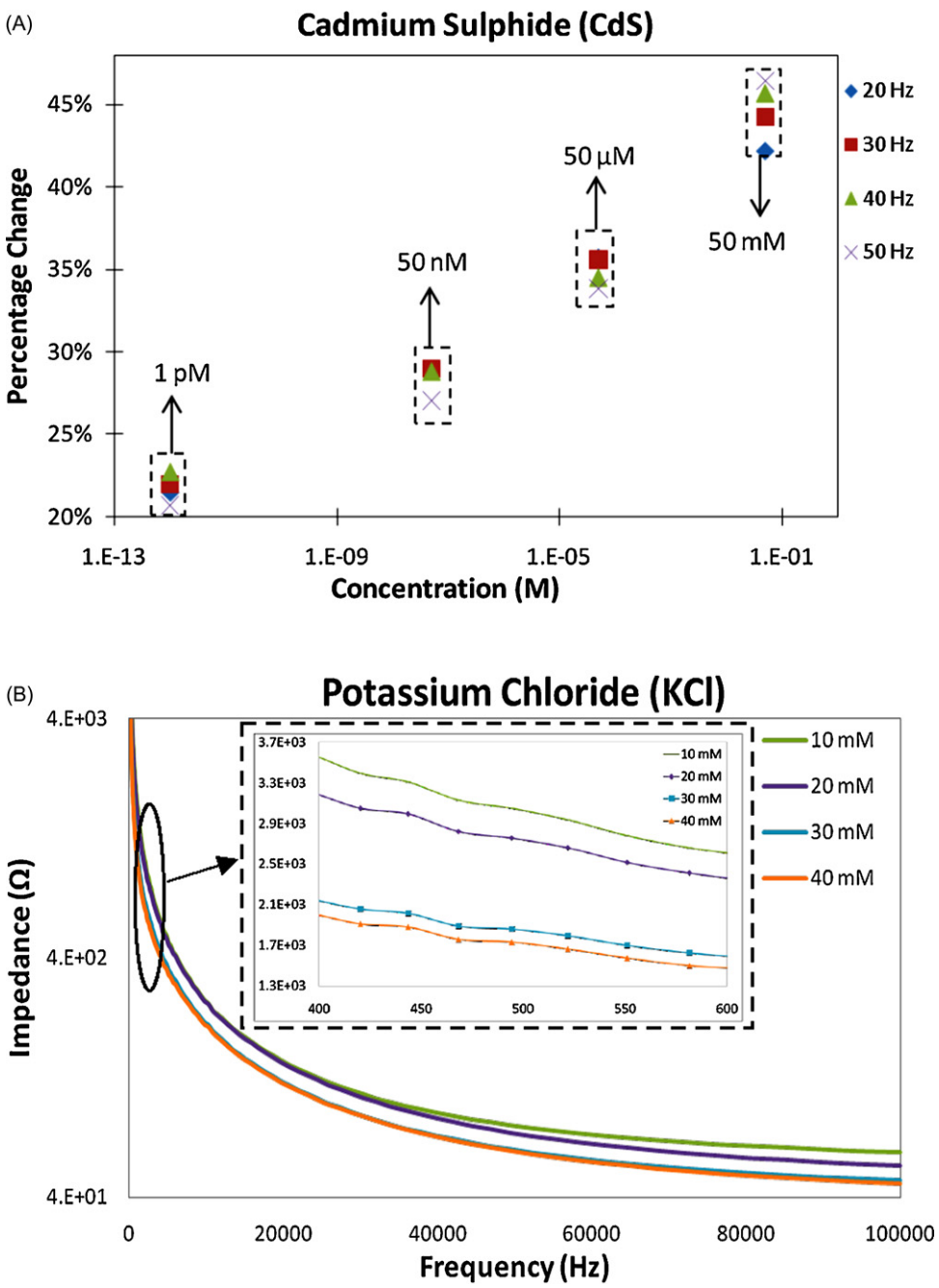

Fig. 3. Sensor response to (A) CdS and (B) KCl at applied potential of 1 mV, inset represents frequency response from 400 Hz to 600 Hz.

(Fig. 1A); i.e. curves under which a certain amount of current is flowing. For example, for electrode widths and spacing of 200 nm, 80% of the current flows in a layer not higher than 200 nm above the surface.

Fig. 1B shows the geometry of the interdigitated electrodes which helps in providing a large sensing area. The capacitance relationship for a parallel plate system is given by

$$C = \frac{\varepsilon_0 \varepsilon_r A}{d} \quad (1)$$

where 'C' is the generated capacitance (F) and 'ε_0' is the dielectric constant of free space equal to 8.85 pF/m. The second dielectric constant, 'ε_r', is the relative permittivity for the medium between the two plates and is equal to 1 for air. The overlapping area between the two plates is 'A' and 'd' is the distance between the two plates. From this relationship, increasing or decreasing the length of the electrodes would produce a linear difference in capacitance, whereas, adjusting the spacing between the two plates would result an inverse response. Based upon this approach some initial values for capacitance were calculated as shown in Fig. 1D.

Taking all the above factors into consideration and the fact that the aim of this study is to try to lower the detection limit of the biosensor device, overall device dimensions of 2 cm × 1 cm × 0.05 cm, with Au IDTs that had a spatial periodicity (λ) of 20 µm, interdigitated space of 5 µm, length of 4995 µm and Au layer thickness of 0.1 µm was chosen. The sensor would have 25 pairs of electrodes with an active sensing area of 1.25 mm^2. Based

upon these features the initial capacitance was calculated to be 0.5 pF.

2.3. Biosensor device fabrication

Biosensor fabrication was performed on 4 in. round glass wafers at the Lurie Nanofabrication Facility (LNF) of University of Michigan. (a) Initially, a positive photoresist (SPR220 3.0) was spin-coated on a glass substrate using Suss Micro Tec ACS200 automatic resist coater-developer. (b) Then the resist film was exposed to UV light through the photomask using a Suss Micro Tec MA/BA-6 contact aligner. (c) Evaporation of 10 nm of chromium (Cr) was followed by evaporation of the 100 nm of Au on Enerjet e-beam evaporator from Denton/Lesker. (d) Lift off was then done in a heated Shipley Microposit 1112A device, with sonication. The wafers were then diced on Micro Automation MA6 dicing Saw. A photograph of the fabricated sensor device is shown in Fig. 1C.

2.4. Flow cell fabrication

A flow cell was designed in AutoCAD™ and fabricated using acrylic material. An O-Ring was used in the flow cell with an outer diameter of 7/16 in. and inner diameter of 5/16 in., resulting in a reservoir volume of 78 μl. The O-Ring was placed in a groove designed with a depth of 1050 μm so that the O-Ring exposure would be 537.5 μm high from the electrode surface thereby providing more than 100 times the required height for an optimal 80% current comprisement curve. The inlet port was designed at an angle of 50° with the outlet port for a complete flow of the sample solution through the microfluidic chamber. An axially magnetized set of Neodymium magnets (diameter – 0.25 in.; thickness – 0.375 in.; magnetic strength – 13,200 G) purchased from K & J Magnets, Inc. was incorporated for the efficient closing of the flow cell which results in the tight sealing of the O-Ring around the sensing area of the biosensor.

2.5. Experiment procedure

Before use, the biosensor was cleaned with acetone and distilled water, and then blow dried with pressurized air. All measurements were conducted at room temperature. A syringe pump was connected to the inlet port of the microfluidic flow cell chamber for loading the sample onto the sensing area of the biosensor. An Agilent E4980A precision LCR meter was connected to the biosensor via the SOIC test clips for impedance measurements. Sample solutions with different concentrations of mouse monoclonal IgG, sarcosine, CdS and KCl were then loaded onto the biosensor. The impedance magnitude of the biosensor was measured at frequency ranges between 20 Hz and 1 kHz with a 1 mV voltage excitation. To measure only the impedance of the biosensor, impedance calibration for the wiring and probes was done before the measurements. The measured impedance data was transferred via USB to a PC for post-processing. The microfluidic flow cell chamber was flushed by passing 1 ml distilled water through the chamber twice, which is more than 13 times the microfluidic chamber volume to ensure complete washing to remove any unbonded molecules. At the end of each test, the biosensor was rinsed with distilled water and dried in a stream of pressurized air.

3. Results and discussions

The response of the fabricated biosensor was first tested toward mouse IgG solution. Fig. 2A shows typical response of the biosensor toward different concentrations of mouse monoclonal IgG at frequencies of 400 Hz, 435 Hz, 465 Hz and 500 Hz. In this figure, set 1 corresponds to the measured impedance response to 1 pM and 10 pM, set 2 corresponds to the measured impedance response to 1 nM, 5 nM and 50 nM, and set 3 corresponds to the measured impedance response of 100 μM. It can be seen that measured responses, at operating frequency of 400 Hz, has decreased from 6140 Ω to 5564 Ω to 4619 Ω to 4331 Ω to 4023 Ω to 3682.5 Ω as concentrations of Mouse Monoclonal IgG increased from 1 pM to 10 pM to1 nM to impedance responses displayed a detection limit as low as 1 pM and the ability of the sensor to distinguish among a wider range (micro, nano and pico level) of sample concentrations.

Fig. 2B shows the impedance percentage change at the sarcosine biosensor interface when compared to a solution of PBS. According to US Food and Drug Administration (USFDA), approved domoic acid limit is 20 μM (Lefebvre et al., 2002). Sarcosine is structurally similar to domoic acid which is a main cause of seafood poisoning. Experiments were conducted at various concentration levels of 1 pM, 100 pM, 100 nM, 100 μM and 100 mM of sarcosine. The impedance percentage changes at 20 Hz for sarcosine were 28%, 31%, 32%, 33% and 37%, when compared to PBS levels. At 50 Hz, sarcosine displayed a 25%, 29%, 30%, 31% and 32% percentage change with respect to PBS levels.

Varying concentrations of highly toxic chemicals CdS and KCl were also tested for the sensor response. Fig. 3A shows the impedance percentage change of the sensor towards CdS at frequencies of 10 Hz, 20 Hz, 30 Hz and 50 Hz, respectively. The sensor response showed that impedance percentage change when compared to distilled water was increased from 22% to 29% to 36% to 44% as the concentration increased from 1 pM to 50 nM to 50 μM to 50 mM for CdS. It is worth noting that the approved level of cadmium by the USFDA is 3 μM (Sheets, 1997). Fig. 3B depicts the measured impedances for concentrations of 10 mM, 20 mM, 30 mM and 40 mM of KCl at operating frequency range of 100 mHz to 100 kHz. It can be seen that impedance decreased as the concentration of the solution was increased. As an example, for measurements at 500 Hz frequency, the impedance value decreased by 10%, 39% and 43% for the 20 mM, 30 mM and 40 mM KCl solution, when compared to the 10 mM KCl solution.

The electrochemical impedance spectroscopy (EIS) sensing mechanism is based on the disturbance of charge transfer dynamics between metal electrodes (Suri et al., 2009; Lisdat and Schafer, 2008; Dharuman et al., 2005). Variation in the concentration of test samples causes a change in the number of ions in the electrolyte. The change in measured impedance response of the biosensor can be attributed to this change since the impedance of an electrolyte solution is related to ion concentration at the sensor–analyte interface (Valera et al., 2007; Brewood et al., 2008).

4. Conclusions

In this work we have successfully fabricated an electrochemical biosensor with gold interdigitated electrodes on a glass substrate with 5 μm IDT electrode width and spacing. Also a flow cell, with inlet and outlet ports for the microfluidic chamber, was fabricated using an acrylic material with a reservoir volume of 78 μl. We have demonstrated the feasibility of the biosensor to distinguish among various concentrations of chemical substances like cadmium sulphide, potassium chloride and sarcosine as well as mouse monoclonal IgG. The measured impedance response of the biosensor displayed detection limits as low as 1 pM. Further investigation is underway to better understand the sensing mechanism to help to improve the selectivity of the sensor to a variety of chemicals and biological substances. In addition, implementation of the electrochemical biosensors into an intelligent electrochemical system is also part of our future work.

Acknowledgments

This work has been partially supported by the US Army Grant Nos. WS911QY-07-1-0003 and W911NF-09-C-0135. The authors gratefully acknowledge Dr. Sandrine Martin and Dr. Katharine Beach of University of Michigan for providing access to the Lurie Nanofabrication Facility (LNF). The authors would also like to thank Mr. Thomas Vaalburg for his technical support.

References

Ah, C.S., Yun, Y.J., Lee, J.S., Park, H.J., Ha, D.H., Yun, W.S., 2006. Appl. Phys. Lett. 88 (13), 133116–133119.
Alocilja, E.C., 2008. Chem. Mater. Sci. 4 (15), 335–359.
Antohe, V.A., Radu, A., Tempfli, M.M., Attout, A., Yunus, S., Bertrand, P., Dutu, C.A., Vlad, A., Melinte, S., Temfli, S.M., Piraux, L., 2009. Appl. Phys. Lett. 94 (7), 0731181–0731183.
Atashbar, M.Z., Bejcek, B.E., Singamaneni, S., 2006. IEEE Sens. J. 6 (3), 524–528.
Atashbar, M.Z., Bejcek, B.E., Vijh, A., Singamanenia, S., 2005. Sens. Actuators B 107 (2), 945–951.
Basu, M., Seggerson, S., Henshaw, J., Jiang, J., Del, A., Cordona, R., Lefave, C., Boyle, P.J., Miller, A., Pugia, M., Basu, S., 2004. Glycoconjugate J. 21 (8–9), 487–496.
Bitziou, E., Rudd, N.C., Szunerits, S., Unwin, P.R., in press. J. Electroanal. Chem.
Brewood, G.P., Rangineni, Y., Fish, D.J., Bhandiwad, A.S., Evans, D.R., Solanki, R., Benight, A.S., 2008. Nucl. Acids Res. 36 (15), e98.
Caruso, F., Rodda, E., Furlong, D.N., 1996. Colloid Interface Sci. 178 (1), 104–115.
Chidsey, C.E., Feldman, B.J., Lundgren, C., Murray, R.W., 1986. Anal. Chem. 58 (3), 601–607.
Cohen, A.E., Kunz, R.R., 2000. Sens. Actuators B 62 (1), 23–29.
Dharuman, V., Grunwald, T., Nebling, E., Albers, J., Blohm, L., Hintsche, R., 2005. Biosens. Bioelectron. 21 (4), 645–654.
Feldman, B.J., Murray, R.W., 1986. Anal. Chem. 58 (13), 2844–2847.
Fosdick, L.E., Anderson, J.L., Baginski, T.A., Jaeger, R.C., 1986. Anal. Chem. 58 (13), 2750–2756.
Gerwen, P.V., Laureyn, W., Laureys, W., Huyberechts, G., Beeck, M., Baert, K., Suls, J., Sansen, W., Jacobs, P., Hermans, L., Mertens, R., 1998. Sens. Actuators B 49 (1–2), 73–80.
Haes, A.J., Duyne, R.P.V., 2002. J. Am. Chem. Soc. 124, 10596–10604.
Hu, X., He, Q., Lu, H., Chen, H., 2010. J. Electroanal. Chem. 638 (1), 21–27.
Huffman, M.L., Venton, B.J., 2009. Analyst 134 (1), 18–24.
Kim, J., Bordeanu, A., Pyun, J.C., 2009. Biosens. Bioelectron. 24 (5), 1394–1398.
Lee, S., Anandan, V., Zhang, G., 2008. Biosens. Bioelectron. 23 (7), 1117–1124.
Lefebvre, K.A., Silver, M.W., Coale, S.L., Tjeerdema, R.S., 2002. Mar. Biotechnol. 140 (3), 625–631.
Leuvering, J.H., Thal, P.J., Van der Waart, M., Schuurs, A.H., 1980. Fresenius J. Anal. Chem. 301 (2), 132–134.
Li, J., Yu, J., Lin, Q., 2010. Anal. Lett. 43 (4), 631–643.
Lisdat, F., Schafer, D., 2008. Anal. Bioanal. Chem. 391 (5), 1555–1567.
Lupu, S., Campo, F.J., Munoz, F.X., 2010. J. Electroanal. Chem. 639 (1–2), 147–153.
Mannoor, M.S., James, T., Ivanov, D.V., Beadling, L., Braunlin, W., 2010. Biophys. J. 98 (4), 724–732.
Min, J., Baeummer, A.J., 2004. Electroanalysis 16 (9), 724–729.
Muramatsu, H., Dicks, J.M., Tamiya, E., Karube, I., 1987. Anal. Chem. 59 (23), 2760–2763.
Niwa, O., Morita, M., Tabei, H., 1989. J. Electroanal. Chem. 62 (5), 447–452.
Ochiai, W., Kawai, R., Suzuki, A., Iwaya, M., Amano, H., Kamiyama, S., Akasaki, I., 2009. Phys. Stat. Sol. C 6 (6), 1416–1419.
Qing, W., Liu, X., Lu, H., Liang, G., Liu, K., 2008. Microchim. Acta 160 (1–2), 227–231.
Raina, S., Kang, W.P., Davidson, J.L., 2010. Diamond Relat. Mater. 19 (2–3), 256–259.
Sanderson, D.G., Anderson, L.B., 1985. Anal. Chem. 57 (10), 2388–2393.
Sheets, R.W., 1997. Sci. Total Environ. 197 (1–3), 167–175.
Suri, C.R., Boro, R., Nangia, Y., Gandhi, S., Sharma, P., Wangoo, N., Rajesh, K., Shekawat, G.S., 2009. Trends Anal. Chem. 28 (1), 29–39.
Horiuchi, T., Tabei, H., Morita, M., Niwa, O., 1992. Anal. Chem. 64 (7), 3206–3208.
Tabei, H., Niwa, O., Hoshino, S., Takahashi, M., Horiuchi, T., 1994. Anal. Chem. 66 (7), 3500–3502.
Vamvakaki, V., Chaniotakis, N.A., 2007. Biosens. Bioelectron. 22 (12), 2848–2853.
Valera, E., Azcon, J.R., Rodrıguez, A., Castaner, L.M., Sanchez, F.J., Marco, M.P., 2007. Sens. Actuators B 125 (2), 526–537.
Vo-Dinh, T., Cullum, B.M., Stokes, D.L., 2001. Sen. Actuators B 74 (1–3), 2–11.
Wang, J., Carmon, K.S., Luck, L.A., Suni, I., 2005. Electrochem. Solid State Lett. 8 (8), H61–H64.
Webster, M.S., Timoshkin, I.V., Macgregor, S.J., Mattey, M., 2009. IEEE Trans. Dielectr. Electr. Insul. 16 (5), 1356–1363.
Wong, Y.Y., Ng, S.P., Ng, M.H., Si, S.H., Yao, S.Z., Fung, Y.S., 2002. Biosens. Bioelectron. 17 (8), 676–684.
Xiang, G., Pan, L., Huang, L., Yu, Z., Song, X., Cheng, J., Xing, W., Zhou, Y., 2007. Biosens. Bioelectron. 22 (11), 2478–2484.
Xu, X., Xing, S., Zeng, L., Xian, Y., Shi, G., Jin, L., 2009. J. Electroanal. Chem. Interface Electrochem. 625 (1), 53–59.
Yang, L., 2008. Talanta 74 (5), 1621–1629.
Yi, Y., Park, J.K., 2005. J. Semicond. Technol. Sci. 5 (1), 30–37.
Zaouak, O., Authier, L., Cugnet, C., Castetbon, A., Potin-Gautier, M., 2009. Electroanalysis 21 (6), 689–695.
Zou, Z., Kai, J., Rust, M.J., Han, J., Ahn, H.C.H., 2007. Sens. Actuators A 136 (2), 518–526.